A comparative study of power production using a generic empirical model in a tidal farm

Kabir B. Shariff and Sylvain S. Guillou

Abstract—**This study presents a generic model for estimating the velocity deficit and turbulence intensity in a tidal turbine farm. The proposed model considers a range of ambient turbulence intensity, the rotor diameter-to-depth ratio, and the rotor thrust coefficient in realistic applications. We evaluate the power generation of a large-scale tidal farm composed of 16 turbines in an in-line and staggered configuration in an ideal channel similar to the Alderney Race in the English Channel. The added turbulence effect is taken into account when assessing the velocity deficit in the farm. As supported by previous studies, the results show that the staggered array produces more power than the rectilinear array. The staggered arrangement benefits from flow acceleration and wide turbine spacing, which improves wake recovery. According to the results, the farm can be resized by decreasing the lateral spacing in the rectilinear array and decreasing the longitudinal spacing in the staggered array without affecting the farm's efficiency. The reduction in farm size will reduce cable costs and provide an opportunity for future expansion. For the tidal turbines in shallow water regions, the ratio of rotor diameter to depth is shown to affect the power generated by the turbines. The power produced in the farm decreases with an increase in the rotor diameter-to-depth ratio due to the limited wake expansion along the vertical plane. This low-computational model can be useful in studying the wake interaction of tidal turbine parks in different configurations.**

Index Terms—**Tidal farm, empirical model, added turbulence, actuator disc, power**

I. Introduction

OVER the last decade, the tidal energy industry has recorded successful deployment and testing of full-scale Tidal Stream Turbines (TST) at dedicated test sites with single units reaching up to 1 MW output [1]. TST is seeing a convergence in technology with the majority of devices being developed being horizontal axis turbines (HAT). For example, [2] reported that as of 2020, over 80% of the active tidal stream devices underwater are HAT. This industrial preference for HAT results from matured technology of aesthetically similar wind turbines, economics, and its high efficiency. The next step towards commercialization is the investigation of the turbine wake interaction in the tidal array as depicted in Figure 1. The wake is a region of disturbed flow behind a turbine that is associated with a decrease in flow velocity and an increase in turbulence. The wake induced on the downstream turbine can reduce the output power and undermine the structural integrity of turbine blades.

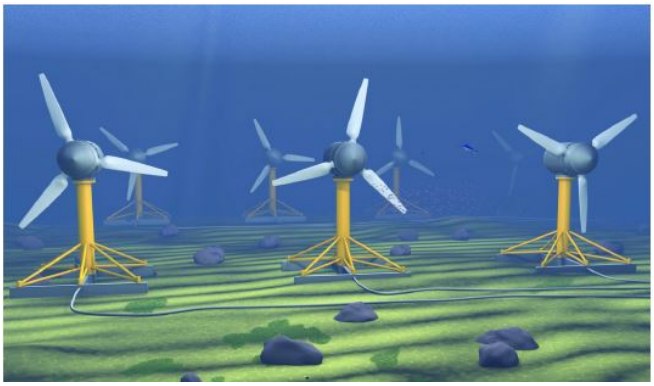

Fig. 1: Illustration of TST farm layout. © Bureau Veritas

Multiple studies have been dedicated to investigating the wake effect in tidal farms with an emphasis on velocity deficits. For instance, Nobel et al. [3] experiment reported an increase in power extraction by three scaled turbines in a staggered array. This results from flow acceleration between the closely-spaced turbine upstream. Mycek et al. [4] shows the performance of the downstream turbine in tandem configuration is affected at low ambient turbulence. Furthermore, the effect of rotor diameter to depth (DH) ratio has been studied [5]. The limited wake expansion along the vertical plane may also affect the power produced by the turbine downstream. As the reduced models provide notable results, yet do not correctly replicate the complexity of full-scale tidal turbines.

In addition, high-fidelity numerical simulation of wake interaction in the tidal park has been carried out by several authors using different turbine representations particularly the Actuator Disc Method (ADM) and the Blade Element Momentum Theory (BEMT) [6]–[8]. These studies also show higher energy production occurs at a minimal lateral spacing around 2 - 3 D while maximizing the longitudinal spacing. The minimal lateral spacing can accelerate the flow for the downstream

This work is part of the thesis of K. B . Shariff funded by the Region Normandie and the Communauté d'Agglomération du Cotentin under the HYDROFARMOD project. S. S. Guillou appreciates the Conseil Général de la Manche and the Interreg VA France (Channel) England Programme for financing the TIGER project.

K. B. Shariff is a doctoral student of Université de Caen Normandie in Laboratoire Universitaire des Sciences Appliquées de Cherbourg (LUSAC). (e-mail: kabir-bashir.shariff@unicaen.fr)

S. S. Guillou is a professor at Université de Caen Normandie and director of LUSAC. 60 rue Max Pol Fouchet, 50130, Cherbourg-Octeville, France(e-mail: sylvain.guillou@unicaen.fr).

Digital Object Identifier:
https://doi.org/10.36688/ewtec-2023-199

turbine whereas the large longitudinal spacing ensures flow recovery. For this reason, the staggered array produces higher energy than the rectilinear array with the same number of turbines in a particular site [9]. Although the numerical simulation provides excellent results, the computational cost for large-scale farms is yet expensive.

For this reason, researchers have devised a low computational analytical/empirical model to estimate the turbine wake. These models are developed from self-similar flow characteristics and are mainly used for estimating the far wake region. Over time, the analytical models have evolved from a simple top-hat model [10] to more accurate artificial intelligence (AI) based empirical models [11] to estimate the velocity deficit in the wind farm. These analytical models require calibration for highly turbulent shallow water tidal turbines [12], [13]. However, these models do not take into account the added turbulence in the wake which may be non-negligible depending on the position of the downstream turbine. For this reason, the authors proposed an added turbulence model for a full-scale tidal turbine [14] and later implemented the model in a simple tidal park [15] in an ideal channel with hydrodynamics similar to the Alderney Race.

In this study, the model is generalized to take into account a range of rotor DH ratios, thrust coefficient, and ambient turbulence intensity. The power production at different tidal farm configurations is studied and compared at different turbine rotor DH ratios. The rest of the paper is organized as follows; section II presents the numerical model used to generate the reference data. The generic empirical model is presented in section III. The tidal farm is introduced in section IV, Results are presented and discussed in section V and the paper ends with concluding remarks.

II. Numerical model

A. Actuator Disk model

The tidal turbine rotor is represented by a uniform actuator disc method in OpenFOAM. The ADM replicates the energy extraction by the turbine through a momentum exchange that creates a pressure jump across the disc. The thrust force applied on the disc region is evaluated as Eq. (1):

$$T = \frac{1}{2}\rho K A U_d^2 \tag{1}$$

where ρ is fluid density, K is the resistance coefficient, A is the frontal surface area and U_d is the velocity at the disc location. This approach of simulating tidal turbines proposed by Harrison et al. [16] is used extensively in the literature for studies attentive to far wake region [7], [8], [17]. Details of the numerical model developed and its validation can be found in the previous work of the authors [14], [15].

III. Empirical model

In this section, a generalized low computational model is proposed to estimate the velocity deficit and turbulence intensity in the wake of a turbine.

A. Wake radius model

Previously, the authors [15] proposed a model for estimating the wake radius of the turbine at different ambient turbulence for a DH40 (i.e. 40% rotor diameter to depth ratio). However, in shallow water, the rotor diameter-to-depth ratio affects the turbine wake radius as shown in Figure 2. The wake radius is evaluated using the Full-Width Half Maximum (FWHM) of a standard Gaussian function as presented by the authors in [15]. The generalized wake radius is expressed as Eq. (2):

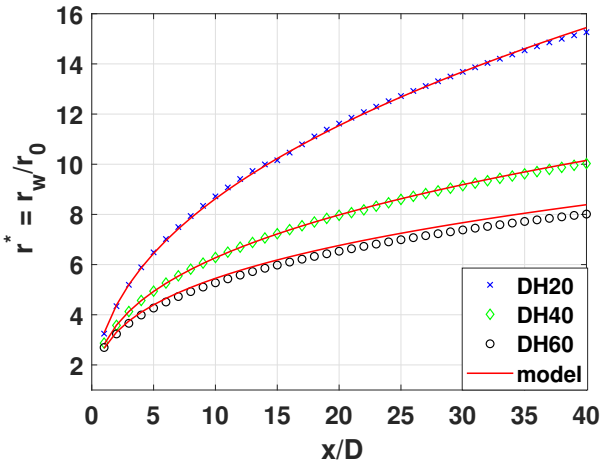

Fig. 2: Comparison of numerical and empirical normalized wake radius at different rotor diameter to depth ratio.

$$r_w = a\left(\frac{x - x_0}{D}\right)^b \tag{2}$$
$$a = 2.36 + 1.834\frac{I_{eff}}{D/H}, \quad b = 0.27\left(\frac{D}{H}\right)^{-0.275}$$

where x, x_0, and D is the downstream distance, the turbine position downstream, and the rotor diameter respectively. The terms a and b are coefficients depending on I_{eff}, the effective turbulence expressed in Eq. (4) and D/H, the rotor diameter-to-depth ratio.

B. Velocity deficit model

To estimate the wake velocity of the tidal turbine, the wake radius model is substituted in the Jensen model [10]. The top-hat shape profile of the Jensen model estimates the average velocity in the wake, however, the numerical data provides the minimum wake velocity in the form of a Gaussian profile. In the present model, we propose to use directly a Gaussian model and then estimate directly the velocity deficit in the wake without using a correction coefficient as proposed by Lo Brutto et al. [18]. The velocity deficit is then expressed as Eq. (3):

$$\frac{\Delta U}{U_\infty} = \left[\frac{\left(1 - \sqrt{1 - C_T}\right)}{\left(\frac{r_w}{r_0}\right)^2}\right] \times \exp\left(-\frac{(y_0 - y)^2 + (z_0 - z)^2)}{r_w^2}\right) \tag{3}$$

where y_0 and z_0 are the turbine coordinates along y, the spanwise and z, the vertical directions, respectively. C_T is the thrust coefficient, r_w is the wake radius downstream and r_0 is the rotor radius. The exponential function provides the Gaussian shape profile along the lateral plane.

C. Turbulence intensity model

The turbulence intensity in turbine wake is expressed by Quarton and Ainsle [19] as:

$$\mathrm{I_{eff}} = \left(\mathrm{I}_0^2 + \mathrm{I}_+^2\right)^{0.5} \tag{4}$$

where I_{eff} is the effective turbulence in the wake, I_0 is the ambient turbulence and I_+ is the added turbulence by the rotor. Assuming the ambient turbulence is stable in the flow, it is, therefore, sufficient to propose added turbulence model to evaluate the turbulence in the flow.

An added turbulence model of a full-scale turbine has been developed by the authors [15]. For a generic model, the added turbulence is expressed in Eq. (5)

$$I_+ = c\left(\frac{x - x_0}{D}\right)^{-d} \times \exp\left(-\frac{(y_0 - y)^2 + (z_0 - z)^2}{r_w^2}\right) \tag{5}$$

$$\mathrm{c} = 0.407\left(\frac{D}{H}\right)C_T^{4.83} + 0.179, \quad d = 0.681 I_0 + 0.472$$

where x_0, y_0, and z_0 are the turbine coordinates along x, the streamwise, y, the spanwise, and z, the vertical directions, respectively. c and d are coefficients relating to non-dimensional rotor diameter to depth ratio (D/H) and the ambient turbulence I_0. C_T is the thrust coefficient, r_w is the wake radius downstream and r_0 is the rotor radius.

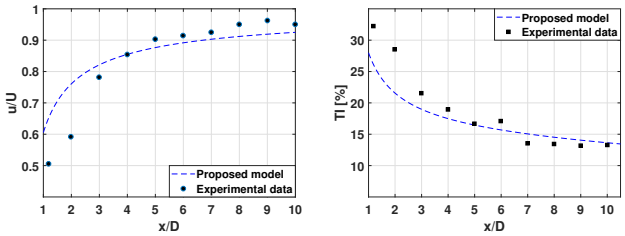

(a) Mycek et al. [20] at 35% DH ratio at 15% ambient turbulence.

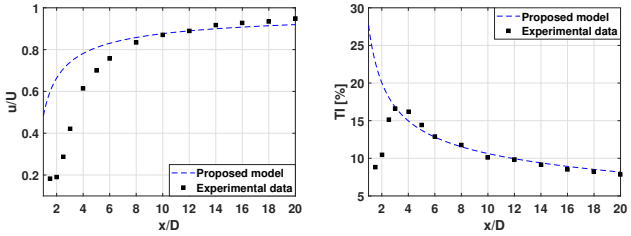

(b) Stallard et al. [21] at 60% DH ratio at 12% ambient turbulence.

Fig. 3: Comparison of the empirical and experimental velocity deficit (left) and turbulence intensity (right) at different rotor DH ratios.

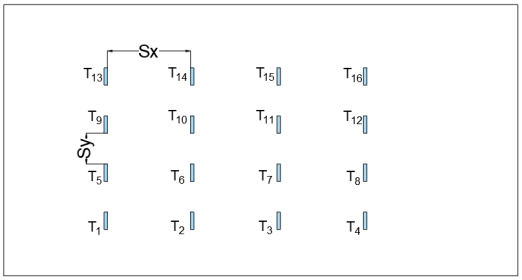

(a) Rectilinear array

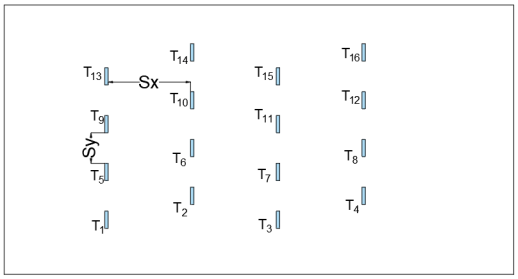

(b) Staggered array

Fig. 4: Schematic of tidal farm array showing different turbine configurations in a farm.

The generic model shows acceptable results in the far wake for the velocity deficit and turbulence intensity compared to experimental data at different rotor DH ratios as shown in Figure 3. Thus, the generalized model can be applied in the turbine park with rather good results in the far wake.

IV. Tidal Farm

In this study, two basic tidal farm configurations rectilinear and staggered comprising N turbines ($N = 16$) in an ideal channel are illustrated in Figure 4. The rotor diameter (D) is 20 m. The choice of turbine size is inspired by the AR2000 Simec-Atlantis TST. The turbines are assumed to perform at Betz operating conditions. The turbine spacing is $S_x = 7D$ and $S_y = 4D$ respectively to ensure flow recovery and benefits from accelerated flow from the upstream turbines. In the ideal farm, the ambient turbulence intensity of 10%, and the mean flow of 2.8 m/s. This hydrodynamic condition is similar to the flow in the Alderney Race [22].

A. Turbine array interaction

In a turbine farm, the wake of the upstream turbine can affect the energy output of the downstream turbine. The evaluation of wake interaction becomes necessary to estimate the energy production on the farm correctly. Different superposition methods have been used in the literature to estimate the wake-turbine interaction [23]. In this paper, the Sum of Square method is used to evaluate the velocity deficit and turbulence intensity in the form of kinetic energy deficit and turbulence energy for the interacting turbines as Eq. (6):

$$\left(1-\frac{u_j}{U}\right)^2=\sum_{ij=1}^{n}\left(1-\frac{u_{ij}}{U}\right)^2\frac{A_{overlap}}{A_0}$$
$$I_{eff}=I_0^2+I_{+,j}^2 \tag{6}$$
$$I_{+,j}^2=\sum_{ij=1}^{n}\left(c\left(\frac{X_{ij}-X_i}{D}\right)^{-d}\right)^2\frac{A_{overlap}}{A_0}$$

where $A_{overlap}$ is the overlap area between the expanded wake area A_w of the upstream turbine and the rotor swept area of the downstream rotor A_0 evaluated in Eq. (7). The three main interactions are illustrated in Figure 5.

The wake overlap area is calculated as follows:

$$A_{overlap}=\begin{cases}0, & if \quad r_w+r_0\leq y\\ A_0, & if \quad r_w-r_0\geq y\\ A_{partial}, & otherwise\end{cases} \tag{7}$$

$A_{partial}$ is the intersecting area between the wake area A_w and the rotor swept area A_0 as shown in Figure 6. The wake intersection area $A_{partial}$ is calculated by [24] as Eq. (8):

$$A_{overlap}=r_w^2\left(\theta_w-\frac{\sin(2\theta_w)}{2}\right)+r_0^2\left(\theta_r-\frac{\sin(2\theta_r)}{2}\right) \tag{8}$$

where θ_w and θ_0 are the angles of the wake intersection arc and rotor intersection arc respectively and can be respectively expressed as:

$$\theta_w=\cos^{-1}\left(\frac{r_w^2+y^2-r_0^2}{2yr_w}\right),\theta_r=\cos^{-1}\left(\frac{r_w^2-y^2-r_0^2}{2yr_0}\right) \tag{9}$$

Figure 7 describes the organigram chart of the generic empirical model. The mean added turbulence intensity at the turbine position is accounted for in evaluating the wake radius hence, the velocity deficit in the farm.

V. Results and discussion

Figures 8 compares the numerical and analytical results at different array configurations. The turbines upstream produced maximum power because they are not affected by the wake interaction. The turbine downstream produces lower power due to the wake interaction in the farm. This is consistent with the numerical results as shown in Figure 8. The power extracted by a turbine is calculated as Eq (10):

$$P_i=\frac{1}{2}\rho C_p A U_i^3 \tag{10}$$

where ρ is the water density, C_P is the power coefficient, A is the cross-sectional area evaluated as $\pi D/4$ and U_i is the incoming velocity for turbine T_i. For the rectilinear configuration, the turbine downstream is fully in the wake of the upstream turbines. The wake interaction is evaluated as presented in Figures 5b. The rectilinear array (Figures 8a and 8c) identify each turbine row independently as having no interaction between turbine rows whereas the staggered configuration shows the wake interaction in both longitudinal and lateral directions as indicated in Figures 8b and 8d. The numerical and empirical power produced by each turbine is compared in Figure 9. In the numerical model, the power is evaluated at a location 1.5 D away from the turbine before the pressure jump begins to develop. The empirical model underpredicts the numerical power in the farm by 2.5%.

A comparison of power produced by each turbine in the rectilinear and staggered array using the empirical model is presented in Figure 10. It is noted that the upstream turbine produces identical power output irrespective of the turbine configuration. For the rectilinear array, the power produces from turbine T_1 - T_4 decreases due to the cumulative wake effect. The downstream turbine is affected by the wake, therefore, producing less power. Similarly, for a staggered array, the turbine downstream produces less power due to the wake effect, however significantly higher than a similar turbine in a rectilinear array. For instance; a turbine T_3 with a double turbine spacing in staggered produces 23.6% more power than a corresponding T_3 in a rectilinear array. The wide turbine spacing allows a substantial recovery velocity deficit in the flow.

The cumulative power produced by N turbines in the farm is evaluated as Eq. (11):

$$P_{farm}=\sum_{j=i}^{N}P_i \tag{11}$$

The total produced in the rectilinear and staggered farm is 22.1 MW and 28.1 MW respectively. For an identical farm size, this study shows the staggered array produces 6 MW power higher than the rectilinear configuration. This is consistent with previous tidal farm studies [6], [7]. The added turbulence effect is higher in the rectilinear configuration as presented in Figure 11. The results show the added turbulence effect is significant in a rectilinear array as a consequence of limited turbine spacing. The turbulence intensity of the turbine downstream in the staggered array is largely recovered due to sufficient turbine spacing. The farm efficiency η_{farm} is defined as the ratio between the total power output from all turbines in a farm P_{farm} and the maximum power P_{farm}^{max} if they operate in unperturbed conditions.

$$\eta_{farm}=\frac{P_{farm}}{P_{farm}^{max}}$$

The farm efficiency for the rectilinear and staggered array is 69.1% and 87.8% respectively.

It is noted that in the in-line configuration, the lateral spacing S_y between turbines row can be reduced without affecting the efficiency of the farm. But, what is the minimal turbine spacing that barely diminishes the output power? The lateral spacing S_y is reduced from $4D$ to $2D$ while maintaining the longitudinal spacing of $7D$ as shown in Figure 12. The cumulative power in the farm remains 22.1 MW for the different lateral spacing. However, a wake interaction effect is spotted between the turbine rows. In reality, there may be some slight difference as the model evaluate the power using the centerline velocity instead of the average velocity across the rotor. In the staggered array, Figure 13

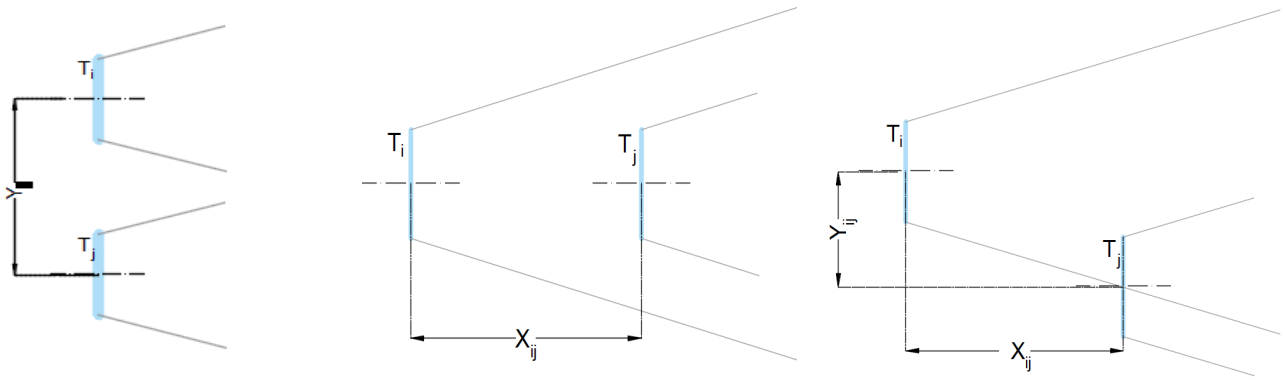

(a) (b) (c)

Fig. 5: Schematic of turbine-wake interaction; (a) no interaction (b) fully immersed and (c) partially immersed in the wake of the upstream turbine.

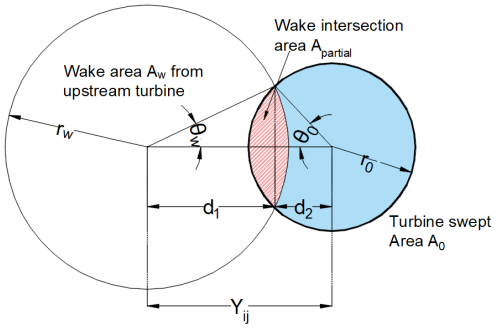

Fig. 6: Partial wake area between a wake effect from the upstream turbine and downstream rotor.

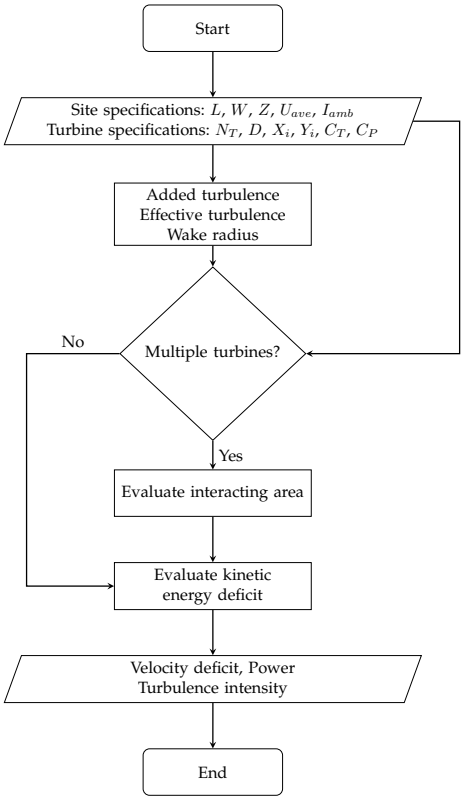

Fig. 7: Organigram chart for the generalized empirical model

compares the velocity contour for longitudinal spacing S_x reduction from $7D$ to $5D$ (i.e. the effective inline spacing is reduced from $14D$ to $10D$). The total power extracted from the farm dropped from 28.1 MW to 27.1 MW. The 3.1% reduction in efficiency can be tolerated in regard to the reduction in the farm size. Reducing the farm size whilst maintaining efficiency is essential because it will drastically reduce cable costs and will present an opportunity for future expansion of the farm.

The effect of the rotor DH ratio is also investigated. The DH ratio is the area the rotor covers along the vertical plane. The rotor wake recovery is affected by the bypass flow. Bypass flow is a region around the turbine with ambient flow conditions. The momentum exchange by the rotor reduces the velocity of flow creating a wake that propagates downstream. Figure 14 shows at a low rotor diameter to depth ratio, the wake expansion is higher and the interaction is higher. The power produced by the downstream turbine decreases with an increase in DH ratio as shown in Figure 15. The total farm power P_{farm} at DH20, DH40, and DH60 is 29.8 MW, 28.1 MW, and 26.9 MW respectively. In a low rotor diameter-to-depth ratio (i.e. DH20), the wake recovery process is faster as the flow in the bypass region is sufficient to cause mixing between the low velocity at the rotor's core and the ambient flow in the bypass region. However, at a high DH ratio (i.e. DH60), the velocity deficit along the rotor is substantial compared to the free stream flow in the bypass region, therefore lagging the wake recovery to the upstream condition. This implies that for an identical turbine size, the power extracted can vary with the channel depth.

VI. Conclusion

This study proposed a generic empirical model to predict the velocity deficit and turbulence intensity in turbine farms. The new model account for wake added turbulence intensity effect and the wake interaction in the farm. Profiting from the turbine arrangement, the staggered array produces about 6 MW power higher than the rectilinear array under the same condition.

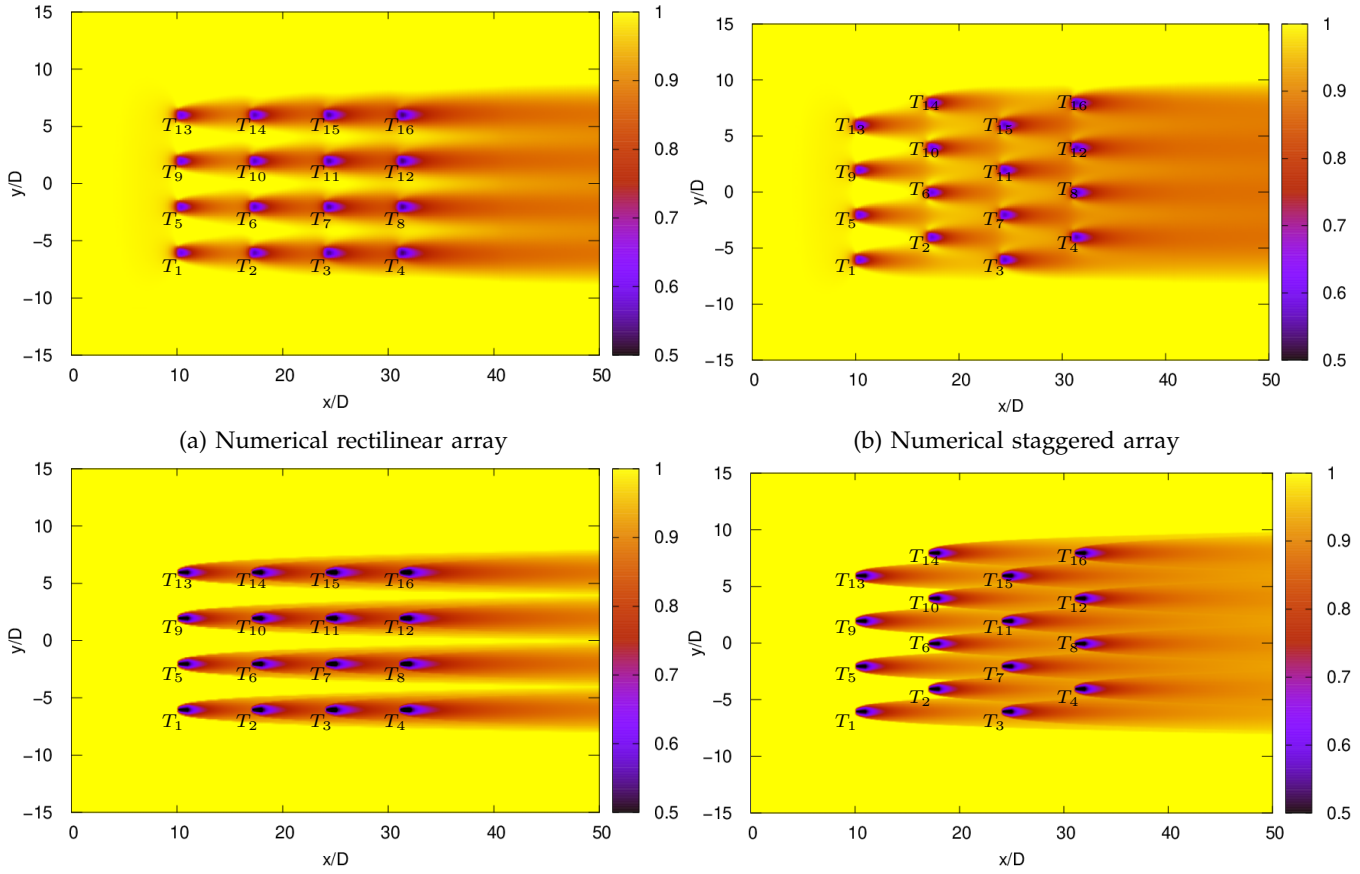

(a) Numerical rectilinear array

(b) Numerical staggered array

(c) Modeled rectilinear array

(d) Modeled staggered array

Fig. 8: Comparison of numerical (top) and modeled (bottom) normalized velocity contour in rectilinear and staggered array configuration in a farm at DH40.

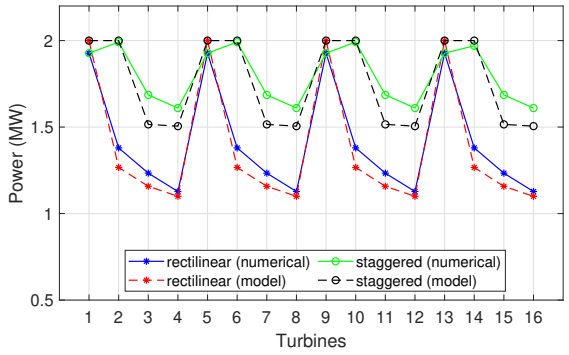

Fig. 9: Comparison of numerical (solid line) and empirical (dash line) power produced by turbines in rectilinear and staggered array at DH40.

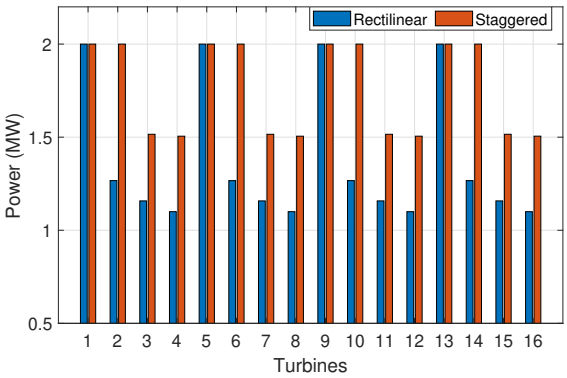

Fig. 10: Power produced by turbines at different array configurations evaluated using the empirical model in the farm at DH40.

The increase in power is attributed to sufficient wake recovery in the former configuration. The comparison with different turbine spacing has shown that the rectilinear and staggered array can benefit from reduced lateral and longitudinal spacing without affecting the efficiency of the farm. Also, the result obtained shows that in shallow water, the channel depth can affect the overall power production in a farm. An increase in power is observed at DH20, this results from sufficient wake expansion at a low rotor diameter-to-depth ratio. The power produces in the farm considered here is at 10% ambient turbulence. An increase in turbulence enhance recovery which may allow harnessing more power [25]. This generic model can provide insight into the power production in tidal farms under different conditions. The effect of ambient conditions on the turbine farm will be presented in the subsequent work of the authors. The next step is to validate the model with a full-scale pilot farm and then optimize the turbine position for maximum power production using a multi-objective algorithm.

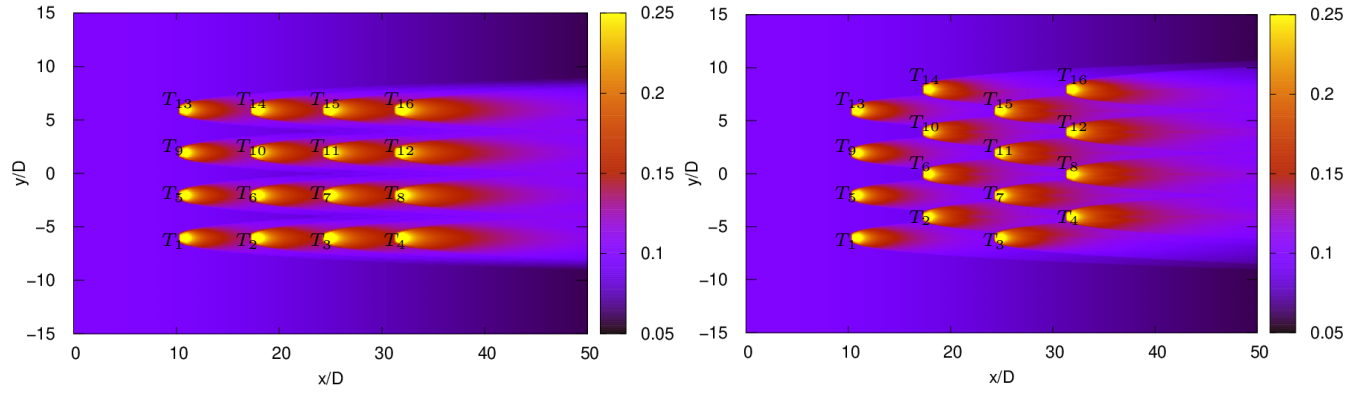

(a) rectilinear array (b) staggered array

Fig. 11: Normalized turbulence intensity contour at different array configurations at DH40.

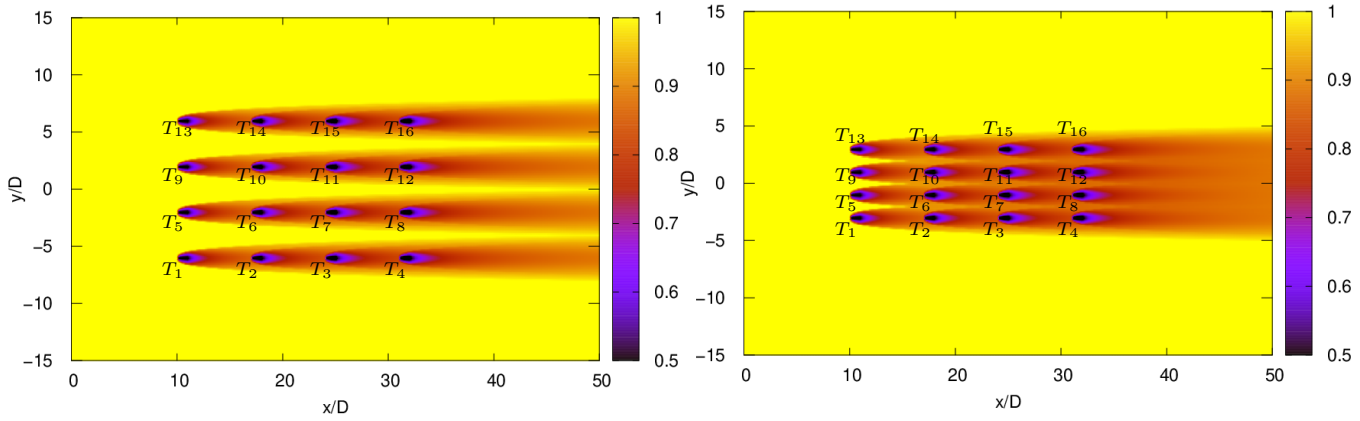

(a) Lateral spacing $S_y = 4D$ (b) Lateral spacing $S_y = 2D$

Fig. 12: Comparison of normalized velocity contour at a different lateral spacing in rectilinear array at DH40.

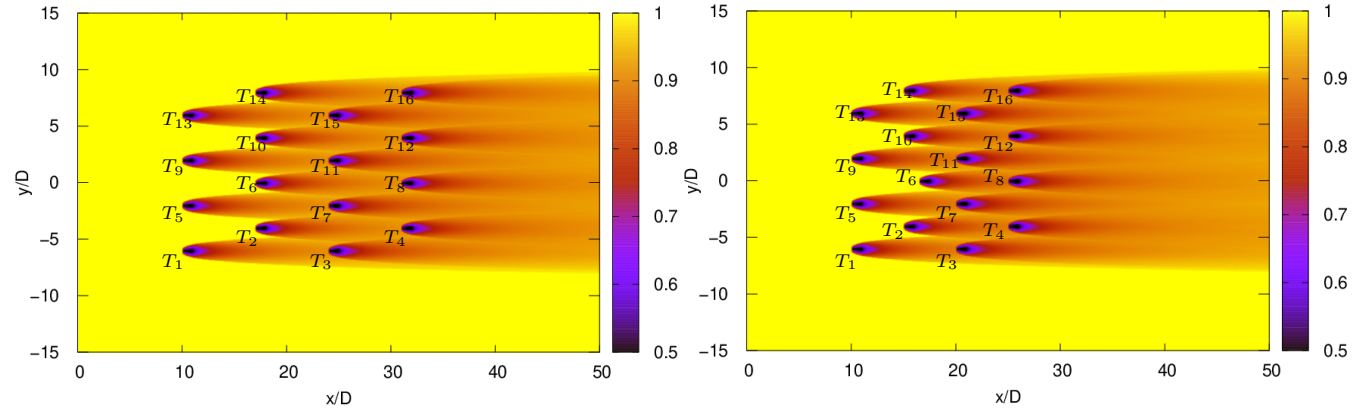

(a) Longitudinal spacing $S_x = 7D$ (b) Longitudinal spacing $S_x = 5D$

Fig. 13: Comparison of normalized velocity contour at a different longitudinal spacing in staggered array at DH40.

ACKNOWLEDGEMENT

The authors thank the Centre Régional Informatique et d'Applications Numériques de Normandie (CRIANN) for providing computing resources.

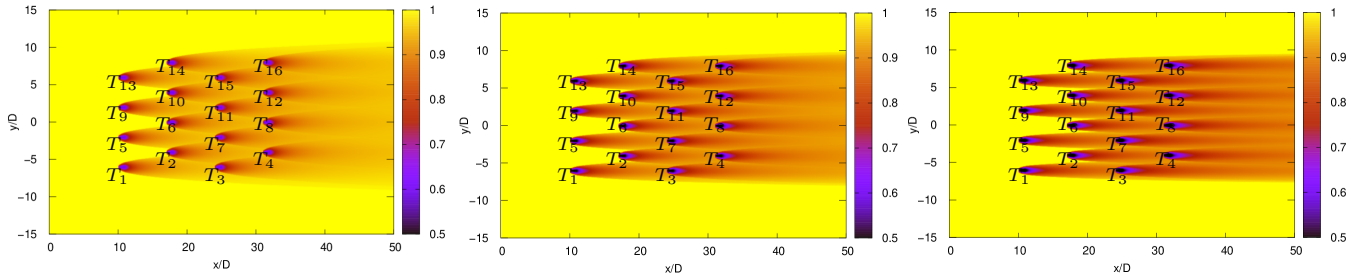

(a) DH20 (b) DH40 (c) DH60

Fig. 14: Comparison of normalized velocity contour at different rotor diameter to depth ratio in staggered array at 7 D turbine spacing.

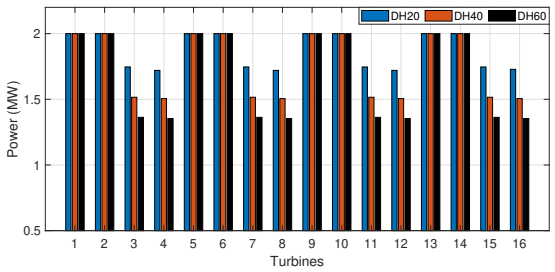

Fig. 15: Power produced by the turbines in staggered array at different rotor diameter to depth ratio using the empirical model.

REFERENCES

[1] EMEC, "Tidal clients : EMEC: European Marine Energy Centre," 2022. [Online]. Available: https://www.emec.org.uk/about-us/our-tidal-clients/

[2] IRENA, "Innovation outlook: Ocean energy technologies," Tech. Rep., 2020.

[3] D. R. Noble, S. Draycott, A. Nambiar, B. G. Sellar, J. Steynor, and A. Kiprakis, "Experimental Assessment of Flow, Performance, and Loads for Tidal Turbines in a Closely-Spaced Array," *Energies*, vol. 13, no. 8, p. 1977, Jan. 2020, number: 8 Publisher: Multidisciplinary Digital Publishing Institute.

[4] P. Mycek, B. Gaurier, G. Germain, G. Pinon, and E. Rivoalen, "Experimental study of the turbulence intensity effects on marine current turbines behaviour. Part II: Two interacting turbines," *Renewable Energy*, vol. 68, pp. 876–892, Aug. 2014.

[5] Y. Zhang, Z. Zhang, J. Zheng, J. Zhang, Y. Zheng, W. Zang, X. Lin, and E. Fernandez-Rodriguez, "Experimental investigation into effects of boundary proximity and blockage on horizontal-axis tidal turbine wake," *Ocean Engineering*, vol. 225, p. 108829, Apr. 2021.

[6] G. Bai, J. Li, P. Fan, and G. Li, "Numerical investigations of the effects of different arrays on power extractions of horizontal axis tidal current turbines," *Renewable Energy*, vol. 53, pp. 180–186, May 2013.

[7] V. T. Nguyen, A. Santa Cruz, S. S. Guillou, M. N. Shiekh Elsouk, and J. Thiébot, "Effects of the Current Direction on the Energy Production of a Tidal Farm: The Case of Raz Blanchard (France)," *Energies*, vol. 12, no. 13, p. 2478, Jun. 2019.

[8] N. Djama Dirieh, J. Thiébot, S. Guillou, and N. Guillou, "Blockage Corrections for Tidal Turbines—Application to an Array of Turbines in the Alderney Race," *Energies*, vol. 15, no. 10, p. 3475, Jan. 2022, number: 10 Publisher: Multidisciplinary Digital Publishing Institute.

[9] S. R. Turnock, A. B. Phillips, J. Banks, and R. Nicholls-Lee, "Modelling tidal current turbine wakes using a coupled RANS-BEMT approach as a tool for analysing power capture of arrays of turbines," *Ocean Engineering*, vol. 38, no. 11, pp. 1300–1307, Aug. 2011.

[10] N. O. Jensen, "A note on wind generator interaction," Risø National Laboratory, Roskilde, Denmark, Tech. Rep. 2411, 1983.

[11] Z. Ti, X. W. Deng, and M. Zhang, "Artificial Neural Networks based wake model for power prediction of wind farm," *Renewable Energy*, vol. 172, pp. 618–631, Jul. 2021.

[12] O. A. Lo Brutto, J. Thiébot, S. S. Guillou, and H. Gualous, "A semi-analytic method to optimize tidal farm layouts – Application to the Alderney Race (Raz Blanchard), France," *Applied Energy*, vol. 183, pp. 1168–1180, Dec. 2016.

[13] P. Pyakurel, W. Tian, J. H. VanZwieten, and M. Dhanak, "Characterization of the mean flow field in the far wake region behind ocean current turbines," *Journal of Ocean Engineering and Marine Energy*, vol. 3, no. 2, pp. 113–123, May 2017.

[14] K. B. Shariff and S. S. Guillou, "An empirical wake model accouting for the velocity deficit and turbulence intensity in a simple tidal park," in *18è Journées de l'Hydrodynamique*, Poitiers, Nov. 2022.

[15] K. B. Shariff and S. Guillou, "An empirical model accounting for added turbulence in the wake of a full-scale turbine in realistic tidal stream conditions," *Applied Ocean Research*, vol. 128, p. 103329, Nov. 2022.

[16] M. E. Harrison, W. M. J. Batten, L. E. Myers, and A. S. Bahaj, "Comparison between CFD simulations and experiments for predicting the far wake of horizontal axis tidal turbines," *IET Renewable Power Generation*, vol. 4, no. 6, pp. 613–627, Nov. 2010, publisher: IET Digital Library.

[17] J. Thiébot, P. Bailly du Bois, and S. Guillou, "Numerical modeling of the effect of tidal stream turbines on the hydrodynamics and the sediment transport – Application to the Alderney Race (Raz Blanchard), France," *Renewable Energy*, vol. 75, pp. 356–365, Mar. 2015.

[18] O. A. Lo Brutto, V. T. Nguyen, S. S. Guillou, J. Thiébot, and H. Gualous, "Tidal farm analysis using an analytical model for the flow velocity prediction in the wake of a tidal turbine with small diameter to depth ratio," *Renewable Energy*, vol. 99, pp. 347–359, Dec. 2016.

[19] D. C. Quarton and J. F. Ainslie, "Turbulence in Wind Turbine Wakes," p. 10, 1990.

[20] P. Mycek, B. Gaurier, G. Germain, G. Pinon, and E. Rivoalen, "Experimental study of the turbulence intensity effects on marine current turbines behaviour. Part I: One single turbine," *Renewable Energy*, vol. 66, pp. 729–746, Jun. 2014.

[21] T. Stallard, R. Collings, T. Feng, and J. Whelan, "Interactions between tidal turbine wakes: experimental study of a group of three-bladed rotors," *Philosophical Transactions of the Royal Society A: Mathematical, Physical and Engineering Sciences*, vol. 371, no. 1985, p. 20120159, Feb. 2013, publisher: Royal Society.

[22] M. Thiébaut, J.-F. Filipot, C. Maisondieu, G. Damblans, C. Jochum, L. F. Kilcher, and S. Guillou, "Characterization of the vertical evolution of the three-dimensional turbulence for fatigue design of tidal turbines," *Philosophical Transactions of the Royal Society A: Mathematical, Physical and Engineering Sciences*, vol. 378, no. 2178, p. 20190495, Aug. 2020.

[23] G.-W. Qian and T. Ishihara, "Wind farm power maximization through wake steering with a new multiple wake model for prediction of turbulence intensity," *Energy*, vol. 220, p. 119680, Apr. 2021.

[24] S. Pookpunt and W. Ongsakul, "Optimal placement of wind turbines within wind farm using binary particle swarm optimization with time-varying acceleration coefficients," *Renewable Energy*, vol. 55, pp. 266–276, Jul. 2013.

[25] T. Ebdon, M. J. Allmark, D. M. O'Doherty, A. Mason-Jones, T. O'Doherty, G. Germain, and B. Gaurier, "The impact of turbulence and turbine operating condition on the wakes of tidal turbines," *Renewable Energy*, vol. 165, pp. 96–116, Mar. 2021.